

Pentad Evolution of the 1988 Drought and 1993 Flood over the Great Plains: An NARR Perspective on the Atmospheric and Terrestrial Water Balance

SCOTT J. WEAVER* AND ALFREDO RUIZ-BARRADAS

Department of Atmospheric and Oceanic Science, University of Maryland, College Park, College Park, Maryland

SUMANT NIGAM

Department of Atmospheric and Oceanic Science, and Earth System Science Interdisciplinary Center, University of Maryland, College Park, College Park, Maryland

(Manuscript received 17 June 2008, in final form 27 March 2009)

ABSTRACT

The evolution of the atmospheric and land surface states during extreme hydroclimate episodes over North America is investigated using the North American Regional Reanalysis (NARR), which additionally, and successfully, assimilates precipitation. The pentad-resolution portrayals of the atmospheric and terrestrial water balance over the U.S. Great Plains during the 1988 summer drought and the July 1993 floods are analyzed to provide insight into the operative mechanisms including regional circulation (e.g., the Great Plains low-level jet, or GPLLJ) and hydroclimate (e.g., precipitation, evaporation, soil moisture recharge, runoff).

The submonthly (but supersynoptic time scale) fluctuations of the GPLLJ are found to be very influential, through related moisture transport and kinematic convergence (e.g., $\partial v/\partial y$), with the jet anomalies in the southern plains leading the northern precipitation and related moisture flux convergence, accounting for two-thirds of the dry and wet episode precipitation amplitude. The soil moisture influence on hydroclimate evolution is assessed to be marginal as evaporation anomalies are found to lag precipitation ones, a lead-lag not discernible at monthly resolution. The pentad analysis thus corroborates the authors' earlier findings on the importance of transported moisture over local evaporation in Great Plains' summer hydroclimate variability.

The regional water budgets—atmospheric and terrestrial—are found to be substantially unbalanced, with the terrestrial imbalance being unacceptably large. Pentad analysis shows the atmospheric imbalance to arise from the sluggishness of the NARR evaporation, including its overestimation in wet periods. The larger terrestrial imbalance, on the other hand, has its origins in the striking unresponsiveness of the NARR's runoff, which is underestimated in wet episodes.

Finally, the influence of ENSO and North Atlantic Oscillation (NAO) variability on the GPLLJ is quantified during the wet episode, in view of the importance of moisture transports. It is shown that a significant portion (~25%) of the GPLLJ anomaly (and downstream precipitation) is attributable to NAO and ENSO's influence, and that this combined influence prolongs the wet episode beyond the period of the instigating GPLLJ.

1. Introduction

The 1988 drought and 1993 flood in the central United States were among the most extreme hydroclimatic events

* Current affiliation: NOAA/Climate Prediction Center, Camp Springs, Maryland.

Corresponding author address: Dr. Scott J. Weaver, Climate Prediction Center, NOAA/NWS/NCEP, 5200 Auth Rd., Rm. 605, Camp Springs, MD 20746.
E-mail: scott.weaver@noaa.gov

in recent decades. The socioeconomic impacts of these episodes were massive, with a price tag in the tens of billions of dollars (information online at <http://www.ncdc.noaa.gov/oa/reports/billionz.html>) and significant loss to life and property. Agricultural interests were particularly impacted as much of the U.S. farming production occurs in the Great Plains. From a scientific perspective these anomalies are equally impressive as they represent extreme departures from the warm season climatology.

The origins of these hydroclimatic extremes have been extensively investigated. Observational inquiries suggest that the 1993 flood was characterized by a

persistent trough in the lee of the Rocky Mountains maintained by upstream eddy activity, providing favorable conditions for enhanced rainfall over the Great Plains (Bell and Janowiak 1995; Mo et al. 1995, 1997; Trenberth and Guillemot 1996). The situation during the late spring–early summer of 1988, on the other hand, was characterized by large upper-level anticyclonic height anomalies over North America whose main effect was to shift the summer storm track well north of its climatological position, into central Canada (Namias 1991; Trenberth and Branstator 1992; Trenberth et al. 1988).

That these anomalies occurred during significant El Niño (1993) and La Niña (1988) events suggests an instigative role for tropical forcing (Trenberth and Branstator 1992; Trenberth and Guillemot 1996). The forcing of midlatitude summer circulation (and precipitation) anomalies by equatorial Pacific heating anomalies, however, remains a topic of much debate. Modeling experiments have moreover been inconclusive. Tropical SST forcing (Bates and Hoerling 2001; Sud et al. 2003), internal atmospheric forcing (Liu et al. 1998), and soil moisture (Atlas et al. 1993; Bosilovich and Sun 1999; Hong and Kalnay 2002) have all been shown to be important in the modeling of these hydroclimate anomalies. A multi-decadal variation of ENSO's influence on Great Plains summer precipitation, with some epochs exhibiting strong correlation with tropical SSTs while the others (1979–95) show weak correlation, has also been suggested (Hu and Feng 2001).

Although there is no consensus on the origins of the large-scale circulation anomalies associated with these extreme events, the regional hydroclimate impacts are reckoned to be generated through local orographic interaction, meridional shifts of the North American storm track, and modulation of local land–atmosphere interactions. Interestingly, the focus on large-scale circulation anomalies has hindered the development of a high-resolution, evolutionary description of atmospheric and land surface states during these pronounced variability episodes, a description that can potentially clarify the operative regional mechanisms.

The objective of this study is to generate just such a description. A high spatiotemporal resolution description of regional hydroclimate anomalies during the warm seasons of 1988 and 1993 is generated to gain insight into the genesis of these extreme hydroclimate episodes over the Great Plains. The basic descriptions are supplemented by pentad-resolution portrayals of the related atmospheric and terrestrial water balance over the Great Plains.

The high-resolution analysis of hydroclimate variability exploits the recent availability of regional reanalysis over this region—the North American Regional Reanalysis (NARR; Mesinger et al. 2006). This precip-

itation and radiance-assimilating, high-resolution reanalysis was enabled by recent advances in data assimilation and land surface modeling. The 27-yr-long (1979–2005) dataset is proving to be a unique resource for hydroclimate research, given its remarkable assimilation of precipitation.

The larger goal of this study is to connect the canonical monthly resolution analyses of extreme hydroclimate episodes with their synoptic underpinnings. By focusing on the supersynoptic time scale (pentad–weekly), the analysis seeks to identify the contribution of the continental-scale, low-frequency (monthly–seasonal) climate variations on the rapidly evolving regional-scale hydroclimate variability. A pentad-level description of regional circulation features (e.g., the Great Plains low-level jet) and the concurrent land surface state (e.g., soil moisture recharge, evaporation) during the warm seasons of 1988 and 1993 in the promising NARR hydroclimate dataset offers an unprecedented view of the evolution of these dry and wet episodes over the Great Plains, including the influence of the large-scale climate variability modes.

2. Datasets and methodology

The NARR is a 27-yr (1979–2005), consistent, high-resolution dataset that covers the North American domain (Mesinger et al. 2006). The original NARR has a 3-h analysis cycle and 32-km horizontal resolution. The data used here have been regridded to $0.5^\circ \times 0.5^\circ$. There are 13 vertical levels (29 total) below 700 hPa, which is adequate for resolving the prominent regional circulation feature, the shallow GPLLJ. The NARR assimilates direct observations of precipitation over land and adjoining oceanic regions using the upgraded regional Eta Model and related data assimilation system. The precipitation assimilation is shown to be successful under the influence of a two-way interaction with the Noah land surface model (Ek et al. 2003; Mesinger et al. 2006). The moisture flux convergence and precipitable water used here are the column-integrated fields provided by the NARR system. Given the NARR's regional domain, the large-scale circulation fields are obtained, as needed, from the National Centers for Environmental Prediction–National Center for Atmospheric Research (NCEP–NCAR) reanalysis (Kalnay et al. 1996).

Pentad averages (5-day means) are analyzed in this study, unless otherwise noted. The NARR pentads were created by averaging the 3-hourly data, while the NCEP–NCAR reanalysis pentad data were produced from daily means. In leap years, the pentad beginning on 25 February is a 6-day average so as to keep the number of pentads (73) per year consistent throughout

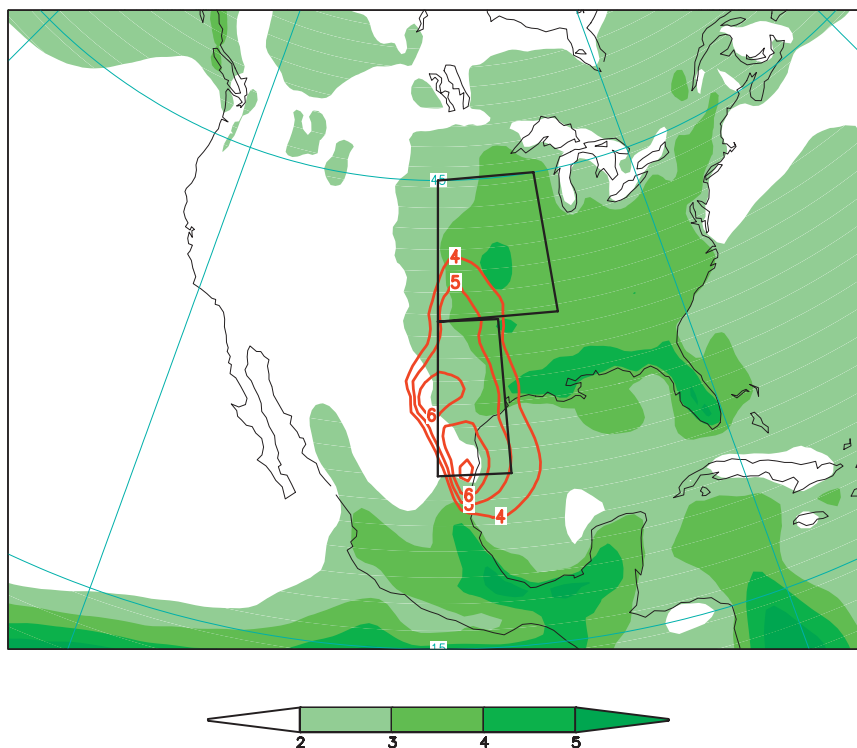


FIG. 1. Seasonal climatology (MJJ) of precipitation (shaded) and the GPLLJ as reflected in the 900-hPa meridional winds (contoured) in the NARR from 1979 to 2005. The northern and southern boxes outline the areas defined by the Great Plains precipitation and low-level jet indices, respectively. Winds $>4 \text{ m s}^{-1}$ are contoured at 1 m s^{-1} intervals and precipitation $>2 \text{ mm day}^{-1}$ is shaded.

the 27-yr NARR record (1979–2005). All anomalies are with respect to their pentad climatology unless otherwise stated.

The analysis is geographically focused on areas exhibiting interesting warm season variability in Great Plains precipitation and of the GPLLJ, which is notable in the latitude bands of 35° – 45° and 25° – 35° N, respectively (Ruiz-Barradas and Nigam 2005, hereafter RBN; Weaver and Nigam 2008, hereafter WN). The correlation between the GPLLJ and precipitation indices in these areas is 0.55 during May–July (MJJ) and 0.71 in July (WN). The precipitation and GPLLJ indices are defined as the area-averaged precipitation and 900-hPa meridional wind anomalies in the 35° – 45° N, 100° – 90° W and 25° – 35° N, 100° – 95° W boxes, respectively. The choice of MJJ as the analysis “season” is made to highlight the overlapping period of these two events: May and June in 1988 and June and July in 1993. Furthermore, in WN it was shown that GPLLJ variations and precipitation are notable during the late spring and early summer.

In RBN and WN, the Great Plains hydroclimate was linked with atmospheric circulation over the adjoining ocean basins, including those related to NAO

and ENSO. The footprints of these “external” climate variability modes in the 1988 drought and 1993 Midwest floods are extracted in section 5 by first computing the linear regression of the NAO and ENSO indices against the NARR precipitation and circulation over the full NARR record. The characteristic patterns, thus obtained, are then multiplied by the NAO and ENSO indices during the drought and flood periods, to uncover the footprints.

Section 3 documents the Great Plains hydroclimatology over the period 1979–2005. Section 4 discusses the atmospheric and terrestrial water balance during the warm seasons of 1988 and 1993. Sections 5 and 6 discuss the NAO and ENSO influences on the Great Plains drought and floods, with concluding remarks following in section 7.

3. Pentad resolution hydroclimate

To put the geographic distribution and magnitude of the 1988 and 1993 hydroclimate anomalies in perspective, Fig. 1 presents the warm season (MJJ) climatology of precipitation (shaded) and the GPLLJ (contoured); the

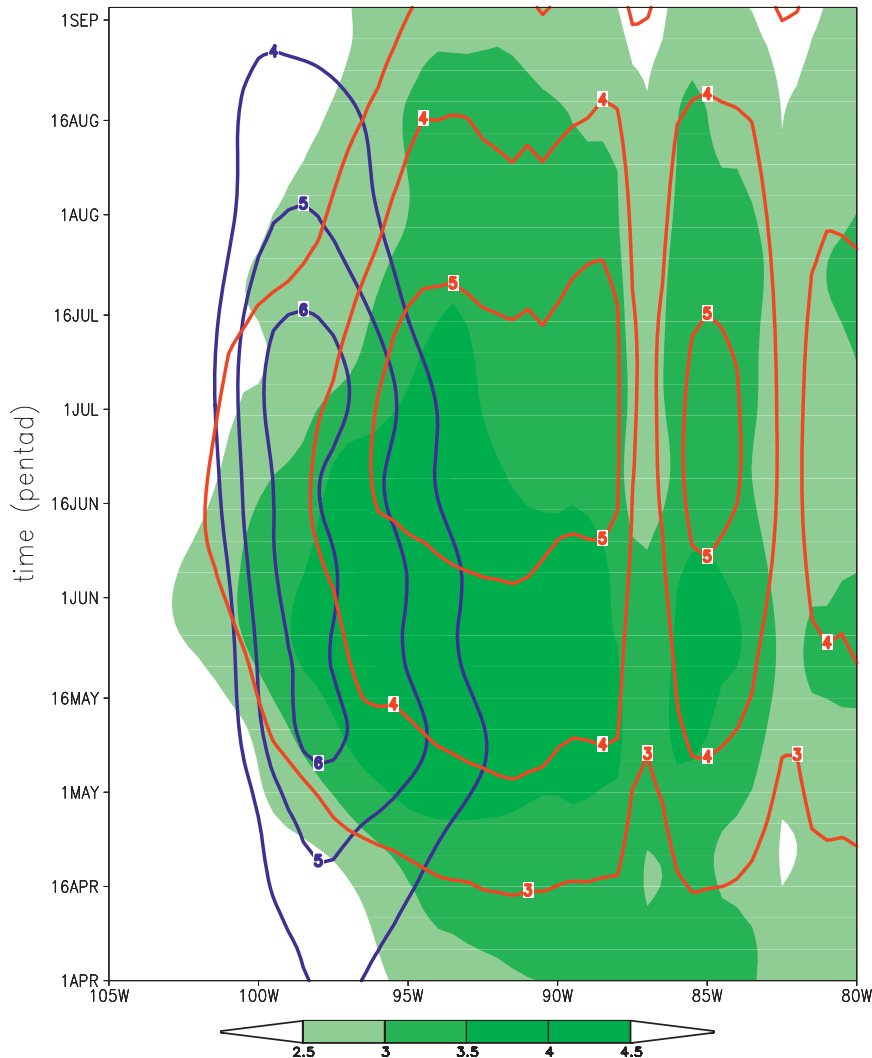


FIG. 2. Warm season climatological (1979–2005) pentad evolution of precipitation (shaded), 900-hPa meridional wind (blue contours), and evaporation (red contours) in NARR. The precipitation and evaporation are meridionally averaged over 35° – 45° N (mm day^{-1}), while the GPLLJ is meridionally averaged over 25° – 35° N (m s^{-1}).

latter from the 900-hPa meridional winds in the NARR. The boxes used to define the precipitation (the northern plains; cf. RBN and section 2) and the GPLLJ (the southern plains; cf. WN and section 2) indices are outlined for reference. These areas have been previously identified as regions of interesting precipitation and GPLLJ variability, respectively (RBN, WN). The boxed areas also include large parts of the expansive precipitation extremum regions in 1988 and 1993 and thus are adequate for a study of these hydroclimate anomalies. Warm season continental precipitation occurs primarily over the eastern half of North America with regional maxima along the U.S. and Mexican Gulf coasts and in the central plains. The GPLLJ is active in a narrow corridor extending from

the northwestern Gulf of Mexico northward toward the continental interior.

Figure 2 shows the 1979–2005 climatological evolution of the meridionally averaged GPLLJ (25° – 35° N), precipitation (35° – 45° N), and evaporation (35° – 45° N) from April to September in the NARR, all at pentad resolution. We perform four applications of 1–2–1 smoothing to remove the influences of temporal striations in the original pentad climatology. The striations (not shown) apparently result from the relatively short NARR data record (i.e., 27 yr) with regard to calculating a pentad time-scale climatology. If NARR were a 100-yr dataset, the striations would most likely be absent.

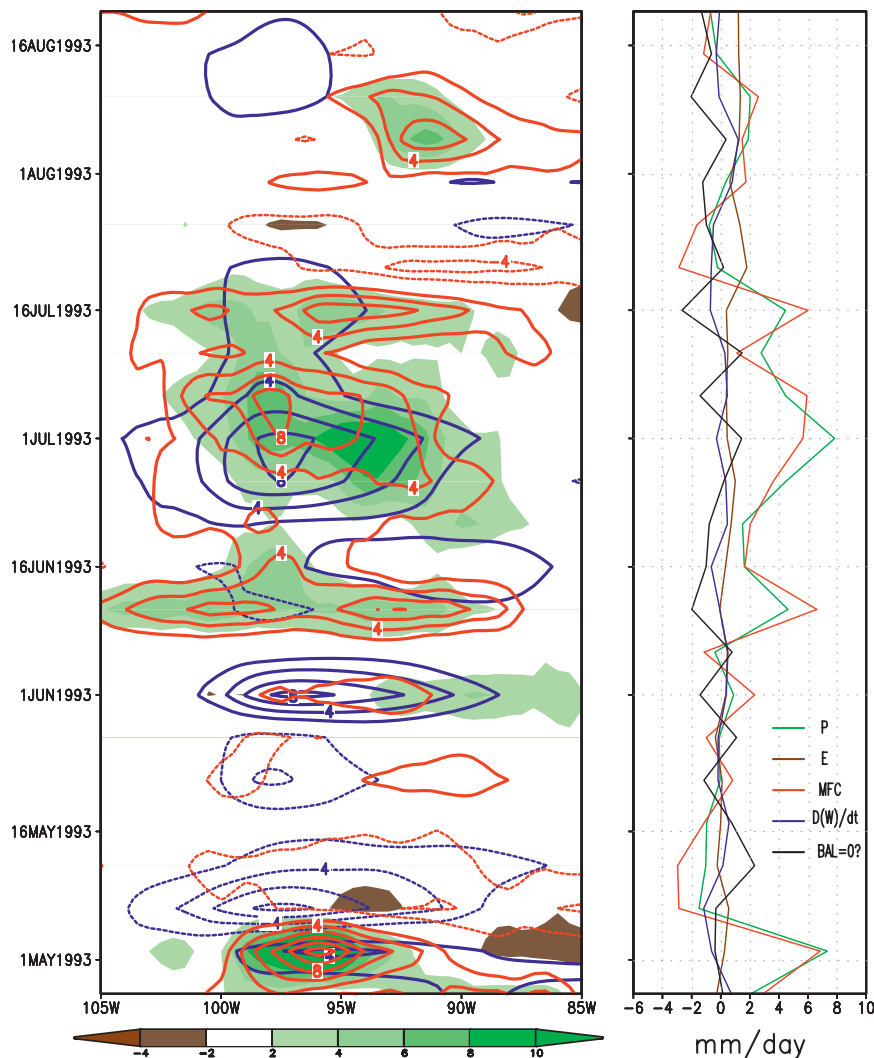


FIG. 3. (left) Pentad evolution of MJJ precipitation (shaded), the GPLLJ (blue contours), and MFC (red contours) anomalies during 1993 in NARR. The precipitation and moisture flux convergence are meridionally averaged over 35° – 45° N (mm day^{-1}), while the GPLLJ is meridionally averaged over 25° – 35° N (m s^{-1}). (right) Corresponding anomalous atmospheric water balance terms given as the area-averaged (25° – 35° N, 90° – 100° W) precipitation (green), evaporation (brown), MFC (red), atmospheric water storage (blue), and the sum (black).

The largest precipitation values are found to the right of the GPLLJ core, indicating the influence of the nocturnally veering LLJs on the location of maximum precipitation (Zhang et al. 2006). It is noteworthy that the GPLLJ retains its maximum value well into July; however, the climatological precipitation is strongest only during May and June. Notable characteristics of evaporation are the time lag with respect to precipitation and the midsummer maximum. Note that evaporation is larger than precipitation over a broad longitudinal range and for a good portion of summer, a well-known feature of U.S. hydroclimatology (e.g., Nigam and Ruiz-Barradas 2006).

4. Hydroclimate anomalies of 1988 and 1993

a. Atmospheric water balance

The improved representation of hydroclimate in the NARR, as compared with the NCEP Global Reanalysis (GR-2; Mesinger et al., 2006), and the presence of both remote circulation and local land surface influences on regional hydroclimate suggests that much can be learned from the analysis of the evolution, including temporal phasing of the key hydroclimate fields in the NARR data. Figures 3 and 4 (left panels) show the latitude-band-averaged evolution of the anomalous precipitation (shaded, 35° – 45° N), 900-hPa meridional

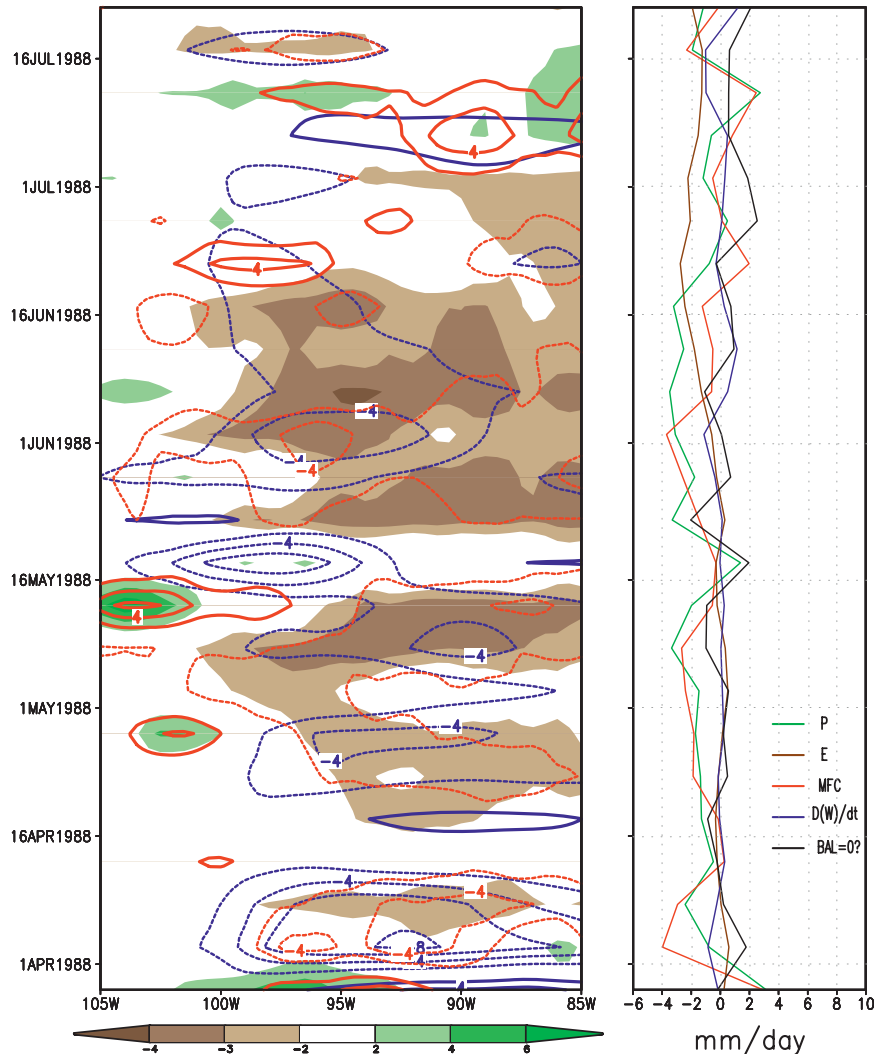


FIG. 4. As in Fig. 3, but for 1988.

winds (i.e., the GPLLJ anomaly; blue contours, 25°–35°N), and moisture flux convergence (red contours, 35°–45°N), while the right panels in the same figures show the evolution of the regional (i.e., area averaged; 35°–45°N, 100°–90°W) atmospheric water balance in the 1993 and 1988 warm seasons, all at pentad resolution.

The vertically integrated moisture equation is $\partial W/\partial t + P - E = \text{MFC}$, where $\partial W/\partial t$ is the change in atmospheric moisture storage defined as the column-integrated water vapor (typically, small), P is precipitation, E is evaporation, and MFC the vertically integrated moisture flux convergence. For 1988, the months of April–June are shown, while in 1993, the May–July evolution is displayed. The period choice reflects the duration of the notable anomalies. Significant positive precipitation anomalies in 1993 occurred during mid- to late June and

early July, with the GPLLJ (blue) leading the moisture flux convergence (red) anomalies by one pentad in the late June to early July episode. The GPLLJ (blue) also appears to lead the maximum precipitation anomaly (as tracked by the 10 mm day⁻¹ precipitation anomaly concurrent with the *termination* of the 8 m s⁻¹ GPLLJ anomaly). As noted earlier within the context of climatology, the precipitation anomaly is right shifted with respect to the GPLLJ anomaly. The anomalous moisture flux convergence, approaching 8 mm day⁻¹, can account for a substantial fraction of the mid-June to early July precipitation excess, when precipitation anomalies are as large as 10 mm day⁻¹.¹

¹ The above-noted temporal phase relationship need not be manifest in all episodes of Great Plains hydroclimate variability.

The 1993 summer hydroclimate (Fig. 3) has other notable features as well: for example, a significant pentaduration GPLLJ episode in early June (and also one in the second week of May) associated with rather modest downstream convergence and precipitation anomalies ($<2 \text{ mm day}^{-1}$).² On the other hand, and interestingly, the notable precipitation anomalies in the first week of May (and mid-June) are not associated with any significant jet variability. It is likely that the low-level convergence accompanying precipitation anomalies in such cases is generated from processes other than kinematic convergence ($-\partial v/\partial y$) in the jet exit region, for example, from local air mass convection or mesoscale convective complex propagation from the Rockies. During this pentad, the large-scale upper-level circulation features exhibited weak anticyclonic height anomalies over the central United States, shifting the upper-level zonal jet and the GPLLJ well into Canada (not shown). This synoptic regime may still exhibit anomalous convective activity (Carbone et al. 2002; Tuttle and Davis 2006) and thus MFC anomalies, even in the absence of significant GPLLJ anomalies, although these large-scale characteristics are more prevalent during the late summer North American monsoon period (Higgins et al. 1997a).

The portrayal of the anomalous atmospheric water balance (Fig. 3, right) clearly shows the dominance of moisture-flux convergence (MFC) in the generation of the precipitation anomalies, with minimal contribution from anomalous evaporation (brown contour). It is somewhat surprising that evaporation is not suppressed during wet episodes, in view of the increased cloudiness and its impact on surface insolation. The atmospheric water imbalance, evaluated as the departure of $(\partial W/\partial t + P - E - \text{MFC})$ from zero, and plotted using the black contour, is also seen to be largest during the wet episodes. Given that $\partial W/\partial t$ is typically small on the pentad time scale (i.e., $P - E \approx \text{MFC}$), the imbalance must arise from errors in E estimation as other terms in the balance (P , MFC) are constrained by observations directly assimilated in the NARR (e.g., precipitation, horizontal winds, and humidity). It is thus not only possible but, perhaps, also reasonable to attribute the atmospheric water imbalance to the lack of evaporation suppression during the wet episodes, that is, to E overestimation at that time. For instance, we find anomalies of $P \approx 4.5$, $E \approx 0$, and $\text{MFC} \approx 6.5$ during the mid-June event in the NARR, leading to an imbalance of -2 mm day^{-1} ;

² This is, perhaps, indicative of a GPLLJ-EOF3 mode of variability, which is characterized by an in-place strengthening of the GPLLJ w.r.t. its climatology and modest enhanced precipitation impacts (see Figs. 10 and 12 in WN).

evaporation suppression (i.e., $E < 0$) would potentially reduce this imbalance.³

Although the evaporation's feedback can be potentially significant, none is likely realized in NARR as this dataset is generated from the assimilation of both synoptic-scale circulation (winds, temperature) and precipitation observations. These powerful observational constraints strongly limit the feedback influence of the evaporation deficiencies during NARR generation, shielding the spatiotemporal evolution of the precipitation and circulation anomalies from potentially corrupting influences. The overestimation of evaporation in the NARR has been noted before within the context of the seasonal evolution of the Great Plains hydroclimate (Nigam and Ruiz-Barradas 2006; A. Ruiz-Barradas and S. Nigam 2008, unpublished manuscript).

The evolution of circulation and precipitation during the 1988 warm season (Fig. 4) is similar in many ways to that in 1993, but for the opposite sign. A striking difference between these summers is the longitudinal range of the precipitation anomalies. The 1988 deficit is over a broad region, extending up to the East Coast (not shown) as opposed to the more focused ($\sim 15^\circ$ longitude spread) wet anomalies in 1993. The disparity in the areal extent of the precipitation footprints is suggestive of a greater role of the GPLLJ—a focused regional feature—in the 1993 wet episode. Instances of precipitation variability generated both with and without the involvement of the GPLLJ however abound in the dry summer case, much as in the wet one. For example, the rainfall deficit in early April follows the substantial weakening of the GPLLJ (and resulting downstream divergence), a classic jet-influenced hydroclimate episode. The major dry episode beginning in late May is however not as clear cut since sizeable rainfall deficits are apparent without significant antecedent jet attenuation, especially in the eastern half of the domain.

Evolution of the area-averaged atmospheric water balance (Fig. 4, right) through the course of the 1988 drought shows a strong relationship between MFC and precipitation, much as in the wet summer (1993). The atmospheric water imbalance during the dry summer is just as pronounced—equaling and sometimes exceeding

³ Note that not all wet-episode imbalances can be reconciled by the suppression of evaporation: the early July wet event, for example, needs increased evaporation to restore balance. Although at odds with the earlier discussion, evaporation can sometimes be enhanced during wet episodes, especially, in those cases with antecedent wetness (e.g., the example in early July), which leads to waterlogged surfaces, or surface ponding. In such situations, evaporation is influenced more by wind speed effects than insolation availability, much as over the oceans.

2 mm day⁻¹—as in the previously discussed wet period. Also, as before, the imbalance can be attributed to the insufficient suppression of near-real-time evaporation in the NARR, as evident from the sluggishness of evaporation in this period. Evaporation does diminish in the NARR but only toward the end of the dry season, that is, much too slowly, from the perspective of the atmospheric water balance. The overly smooth brown curve (E) testifies to this field's sluggishness in the NARR. Were evaporation more responsive, negative anomalies would set in sooner, following the precipitation deficit episodes and leading to a reduced regional water imbalance. It would be interesting to get a reading on the NARR's evaporation from the perspective of the regional terrestrial water balance.

Much can be learned from the inspection of the temporal phasing of 1988 and 1993 anomalous atmospheric water balances (i.e., Figs. 3 and 4). Nevertheless, it is necessary to more objectively assess the lead-lag relationship between the GPLLJ and precipitation during these anomalous seasons, especially given our assertion emphasizing the instigative role of the GPLLJ in producing the precipitation anomalies. To be sure, we present a more objectively defined analysis of the evolution of precipitation and the GPLLJ during the warm seasons of 1988 and 1993. Figure 5 shows the pentad precipitation index (as defined in section 2) lag regressions to precipitation and the GPLLJ from -2 to zero pentads for the seasons of 1988 and 1993 only. For 1988 the analysis includes all pentads from MJJ, while for 1993 only the pentads from 15 June to 30 July are employed. This is consistent with the temporal characteristics of these anomalous hydroclimate episodes (i.e., Figs. 3 and 4).

In general, the temporal phasing in the lagged regression analysis corroborates that from Figs. 3 and 4, which is highlighted by a northward expansion and strengthening of the GPLLJ leading the precipitation anomaly in 1993 (right column) as early as two pentads, as well as a negative GPLLJ anomaly leading the precipitation anomaly by one pentad, with a northward shifted jet coincident with the precipitation anomaly during 1988 (left column). These GPLLJ and precipitation patterns bear remarkable resemblance to GPLLJ EOF modes 1 and 2 from the monthly analysis conducted in WN. However, here we see their expression via regressions obtained including only the pentads of a given season (i.e., 1988 and 1993), attesting to their robustness during these events.

b. Terrestrial water balance

Observational and modeling studies of the 1988 and 1993 hydroclimate events suggest a contributing role for

soil moisture anomalies (Atlas et al. 1993; Bell and Janowiak 1995; Sud et al. 2003). Figures 6 and 7 (left panels) show the pentad evolution of precipitation (shaded), the 0–2-m soil moisture recharge (2 m is the full depth of the Noah soil column), $\partial(\text{SM})/\partial t$ (blue contours), and evaporation (red contours) anomalies during the 1993 and 1988 summers. All quantities here are averaged over 35°–45°N so that the regional terrestrial water balance can be assessed.⁴ The wet and dry summer displays show the terrestrial water budget to be in much greater imbalance than the atmospheric one, given that only about half of the precipitation anomalies can be accounted for at the land surface, principally, by the concurrent recharge of soil moisture. Evaporation accounts for a very small fraction, as it lags precipitation, and accounts for an even smaller one in nature since the NARR's evaporation is deemed excessive from the atmospheric and terrestrial (Nigam and Ruiz-Barradas 2006) water balance perspectives. A reasonable deduction on the origin of the significant terrestrial water imbalance is then the unresponsive runoff in the NARR.⁵

The area-averaged runoff is shown in the right panels in Figs. 6 and 7, and its near-constancy during the evolution of both one of the wettest and driest Great Plains summers is, perhaps, the most striking feature of the regional terrestrial water balance in the NARR. This insensitivity leads to the underestimation of runoff in the wet episodes and its overestimation in the dry ones. Along with evaporation sluggishness, the runoff unresponsiveness can well account for the heightened terrestrial water imbalance in the NARR by as much as 4 mm day⁻¹ in the 1993 summer (Fig. 6).

The pentad resolution display of hydroclimate evolution in these extreme summers suggests, at best, a minor causative role for soil moisture anomalies, as evaporation anomalies lag the precipitation signal by as much as two pentads. This view of the role of soil moisture finds strong support in analyses of the regional atmospheric water balance, where moisture flux convergence (and not local evaporation) is shown to be the dominant contributor to moisture variability. Moisture flux convergence can however arise both from kinematic convergence generated by regional circulation features (e.g., in the GPLLJ exit region, as noted earlier) as well as from larger-scale circulation (and related low-level divergence) anomalies. The potential influence of regional soil moisture

⁴ Soil moisture variations are represented as recharge, that is, $\partial(\text{SM})/\partial t$, where SM is the soil moisture, since the terrestrial water balance is $\partial(\text{SM})/\partial t = P - E - R$, where R is the runoff.

⁵ The imbalance is not attributed to the underestimation of the soil moisture recharge as more recharge would eventually increase evaporation, which is already deemed excessive.

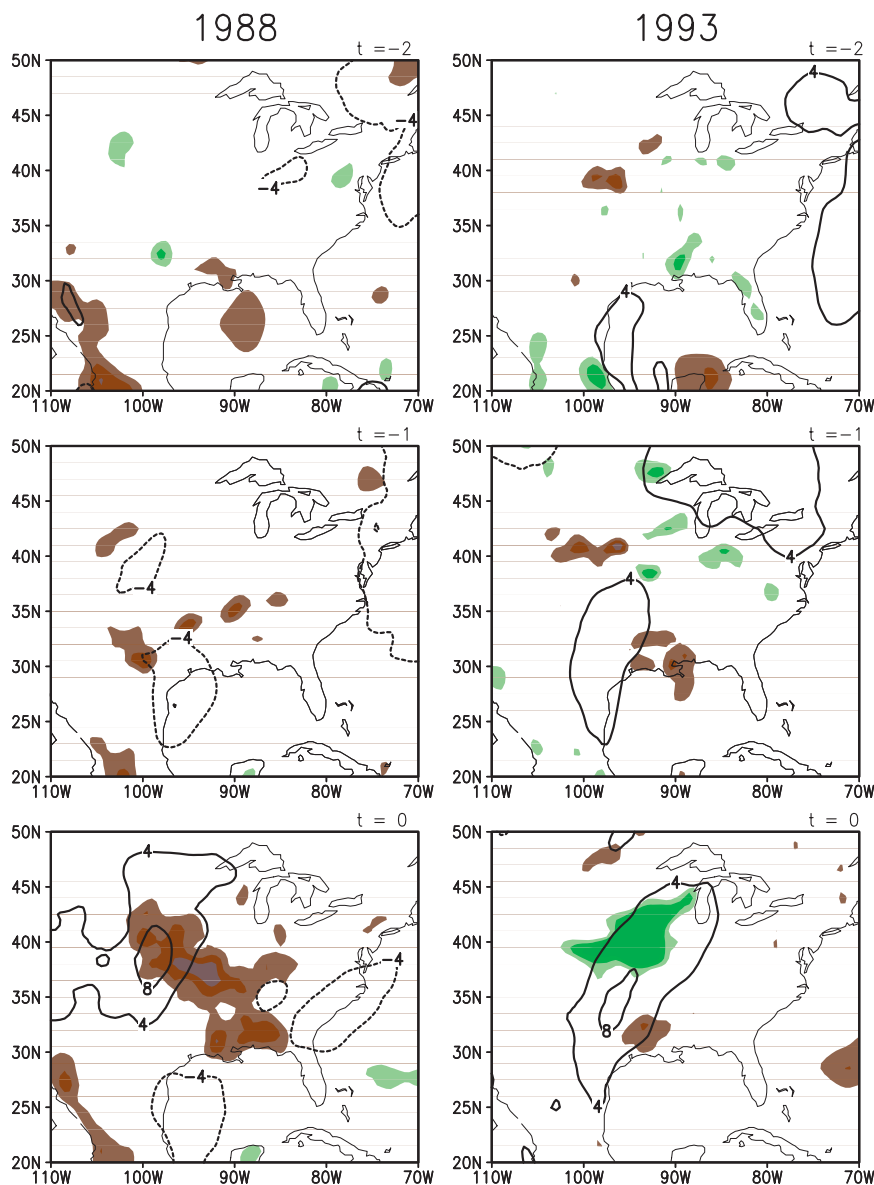


FIG. 5. The evolution of precipitation (shaded) and the GPLLJ (contoured) during MJJ of (left) 1988 and (right) 15 Jun–30 Jul 1993 from -2 to zero pentads as diagnosed through lagged regressions of the Great Plains precipitation index anomalies. The precipitation is shaded at 3 mm day^{-1} intervals beginning at 6 mm day^{-1} . The brown (green) shading represents negative (positive) precipitation anomalies. The GPLLJ is contoured at 4 m s^{-1} .

anomalies on the local thermodynamic environment, including stability, and the resulting impacts on moisture flux convergence are, of course, not explicitly analyzed here.

The contribution of nonlocal evaporation and related moisture advection in the Great Plains hydroclimate evolution was qualitatively assessed from examination of the spatiotemporal structure of evaporation over the fetch region (the southern Great Plains, 25° – 35° N). In mid-June 1993, the precipitation anomaly over the southern plains was comparable to that over the northern

plains, and was followed by a modest evaporation anomaly ($\sim 1 \text{ mm day}^{-1}$) in late June–early July, in sync with the GPLLJ strengthening. The southern plains may thus have been an immediate source of additional moisture for the early July precipitation episode over the northern plains (35° – 45° N), but this increment can account for only 10%–15% of the total precipitation that led to the flooding of the northern plains. An oppositely signed but otherwise similar southern contribution is manifest in the dry episode evolution, in mid-June 1988.

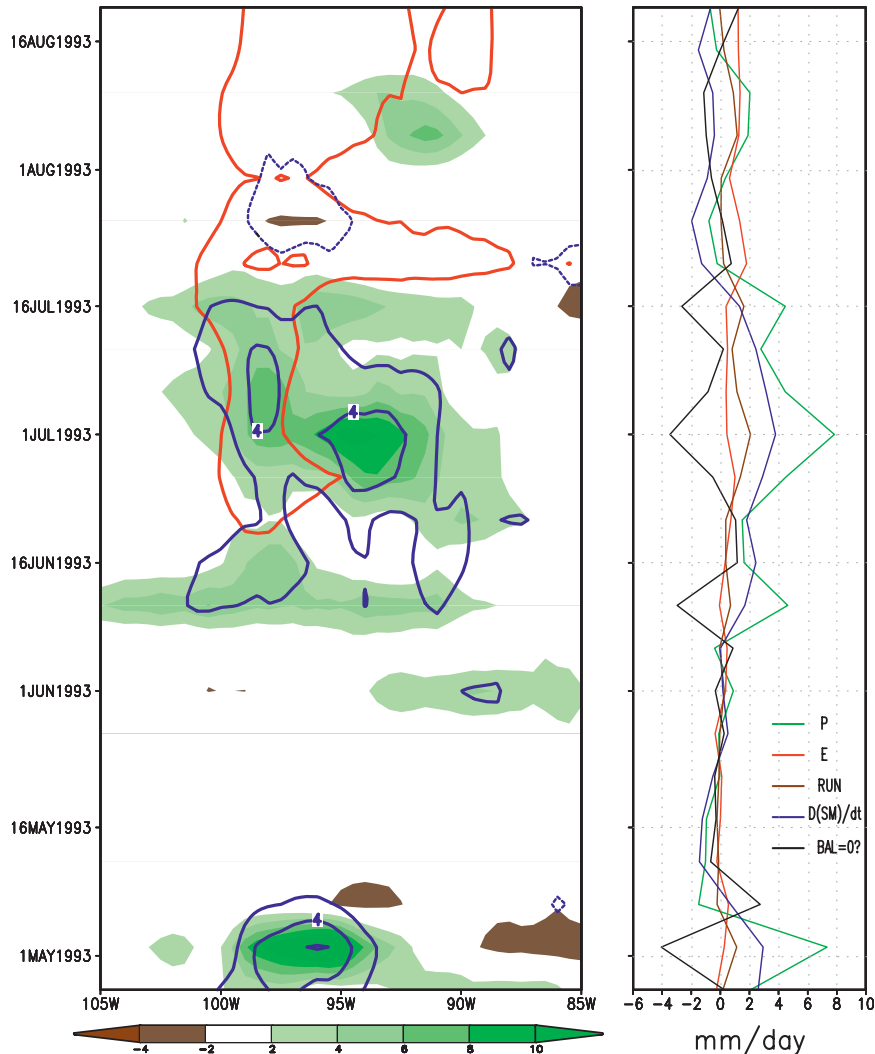


FIG. 6. (left) Pentad evolution of MJJ 35°–45°N meridionally averaged precipitation (shaded), evaporation (red contours), and soil moisture recharge (blue contours) during 1993 in NARR. (right) Corresponding anomalous terrestrial water balance terms given as the area-averaged (35°–45°N, 90°–100°W) precipitation (green), evaporation (brown), runoff (red), soil moisture recharge (blue), and the sum (black). All units are in mm day^{-1} .

The notably marginal contribution of evaporation to the atmospheric column water evident in Figs. 3 and 4, which depict the column budget to be $P \approx \text{MFC}$, and the temporal lagging of evaporation with respect to precipitation at pentad resolution corroborate the findings of Ruiz-Barradas and Nigam (2005, 2006) on the dominance of transported moisture in Great Plains precipitation variability. These authors also showed that most current climate models are quite unrealistic in this regard as coincident evaporation is the dominant moisture source in model simulations of Great Plains hydroclimate variability.

5. Regional circulation and precipitation anomalies

It is of some interest to examine the three-dimensional structure of the regional water vapor conduit from the Gulf of Mexico (the GPLLJ) during extreme hydroclimate episodes, given that related moisture transports are the major contributor to precipitation anomalies over the Great Plains in both 1988 and 1993. The considerable influence of the large-scale circulation on the GPLLJ on supersynoptic to seasonal time scales (Byerle and Paegle 2003; Higgins et al. 1997b; WN) also merits such an examination.

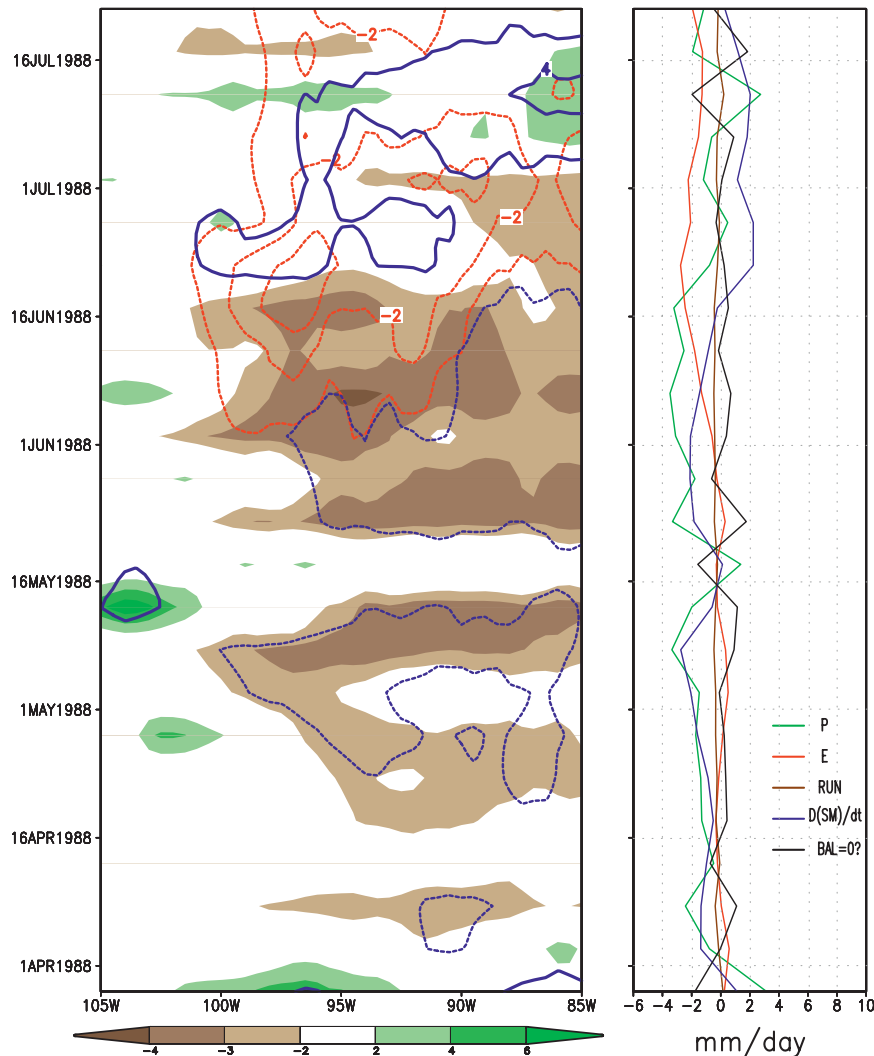


FIG. 7. As in Fig. 6, but for 1988.

Interannual variability of the GPLLJ was examined in WN wherein preferred modes of monthly GPLLJ variability were elucidated. The loading vectors of the first two modes, accounting for a majority of the variance (61% combined), exhibited a meridionally stretched GPLLJ (mode 1) tied to the Gulf of Mexico moisture source and a meridionally displaced (mode 2) GPLLJ disconnected from the Gulf. Both of these GPLLJ structures exhibit profound influence on the structure and amplitude of regional precipitation anomalies.

a. GPLLJ variability

Figure 8 shows the west–east cross section of the latitudinally (25° – 35° N) averaged meridional winds in July 1993 and June 1988; the monthly values (contoured) are

shown atop that month's climatology (shaded) in the top panels. In 1993, the core of the GPLLJ is strengthened (by more than 50%, $\sim 10 \text{ m s}^{-1}$) and vertically stretched; while in 1988, it is shifted westward and is much weaker ($\sim 3 \text{ m s}^{-1}$, i.e., a 50% reduction). The latitudinal reach of the jet in these extreme summer months is shown in the bottom panels of Fig. 8, from a display of the south–north cross section of zonally averaged (102° – 95° W) meridional winds. The nose of the jet is meridionally extended in 1993 while in 1988 there is significant northward displacement of the entire jet core, effectively isolating the jet from its primary moisture source—the Gulf of Mexico. It seems that it is not the lack of the GPLLJ in 1988 that suppressed the moisture fluxes as suggested by the 25° – 35° N domain analysis of jet variability (Fig. 4); however, it is the extreme northward

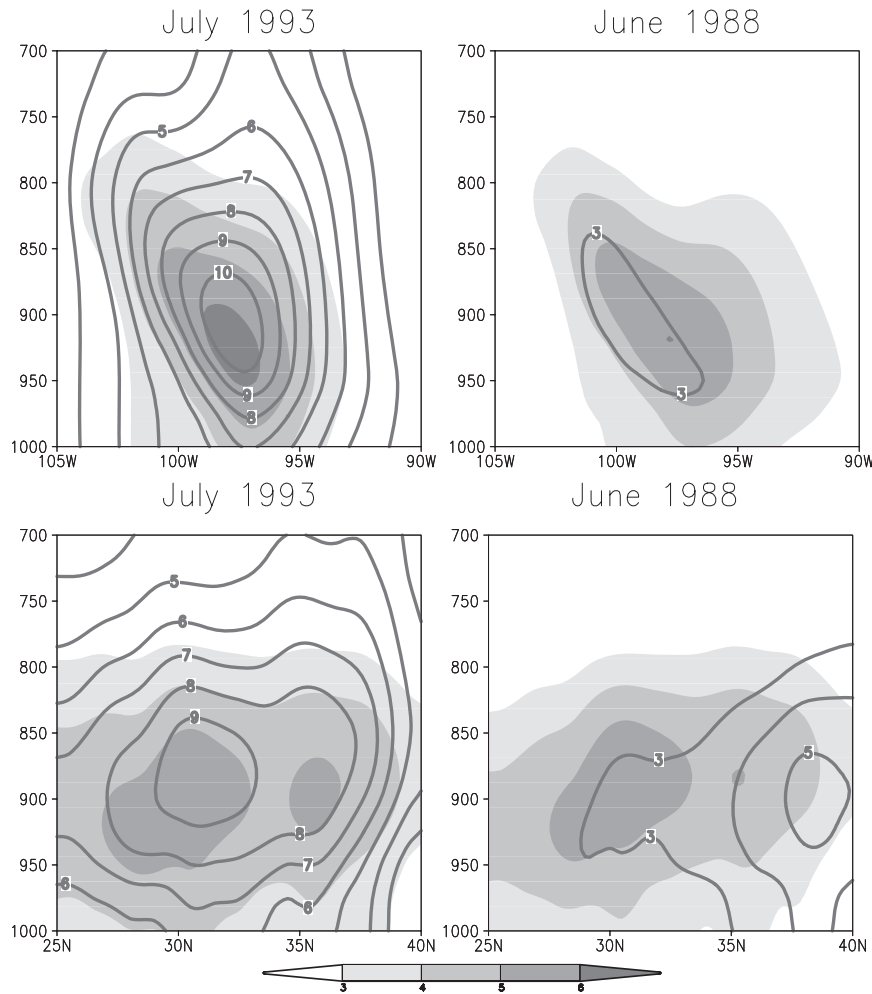


FIG. 8. (top left) West to east cross section of the 25° – 35° N meridionally averaged meridional wind for the July climatology (shaded) and July 1993 (contoured). (top right) As at top left, but for the June climatology (shaded) and June 1988 (contoured). (bottom left) South to north cross section of the 102° – 95° W zonally averaged meridional wind for the July climatology (shaded) and July 1993 (contoured). (bottom right) As at bottom left, but for the June climatology (shaded) and June 1988 (contoured). Units are in m s^{-1} .

position and attendant disconnection from the Gulf that characterize the summer of 1988. The 1988 (meridionally displaced) and 1993 (meridionally stretched) GPLLJ structures are not unlike the characteristic patterns of monthly GPLLJ variability (modes 1 and 2 in WN), which were found to be connected to large-scale circulation variability emanating from the adjoining ocean basins. The same modes did not exhibit significant connectivity to the land surface fields.

b. Great Plains precipitation: Influence of ENSO and NAO

The influence of large-scale circulation variability on regional hydroclimate raises the prospects of predict-

ability and begs the following question: What is the contribution of the leading climate variability modes in the generation of notable precipitation anomalies over the Great Plains? The contributions of the leading Pacific and Atlantic basin modes—ENSO and NAO, respectively—are investigated here. The modes were chosen because of their documented links to Great Plains summer precipitation variability (WN, RBN; see the references therein). While the characteristics of NAO and ENSO variability can clearly be seen in monthly analyses, this does not guarantee that their influence on regional anomalies will be static across the pentads composing a given month. The NAO exhibits significant submonthly variability and frequently switches sign within a month (Benedict et al. 2004; Franzke et al.

2004). Compo et al. (2001) find that there are significant differences in the midlatitude height response to ENSO over the Pacific North American region on the synoptic, submonthly, intraseasonal, and seasonal time scales.

As a case study, we analyze the ENSO and NAO contributions in July 1993 – the recent extremely wet period over central United States. Both the Niño-3.4 and NAO indices were constructed at pentad resolution for the period 1979–97. The ENSO influence was extracted using regressions of the preceding spring's Niño-3.4 SST index, when the ENSO amplitude is still large⁶ and lagged regressions of the May index are used. NAO's influence, on the other hand, was obtained from contemporaneous regressions of the normalized NAO index in view of NAO's intraseasonal time scales.

The NARR precipitation and 900-hPa meridional wind regressions were obtained for the 1979–97 period, using pentads 24–30 (May) in the case of ENSO and pentads 36–42 (July) for the NAO. The modal contributions to the 1993 wet episode were then obtained as the product of the 1993 pentad index values and the corresponding period regression patterns. Figure 8 (top left) shows the evolution of the total precipitation anomaly in the 37°–45°N latitude belt during July 1993.⁷ Positive precipitation anomalies persisted throughout the month; however, the first 10 days exhibited the largest signal. Figure 8 (bottom left) shows the same anomaly after removing the NAO and ENSO contributions. Although the “residual” anomaly is broadly similar to the total anomaly, notable differences are evident in early July, when the anomalies differ by 2–3 mm day⁻¹, that is, by about a fourth. However, the midmonth precipitation anomalies were more significantly impacted, being reduced by more than 3 mm day⁻¹ in some areas.

The modal contributions to the 1993 July precipitation anomaly are shown in the right-hand panels of Fig. 8. The ENSO exhibits significant spatial and temporal stability when compared to the NAO, with the longitudinal gradient being nearly constant and with little temporal evolution. The NAO influence is more variable in contrast, and, interestingly, it is robust immediately after the big early July precipitation event.

⁶ ENSO variability is phase locked to the seasonal cycle, with SST amplitudes peaking in winter and spring (Rasmusson and Carpenter 1982). Given the long ENSO time scale, its influence in other seasons is best extracted using lead-lag regressions of the peak month indices.

⁷ The area covering 37°–45°N was used to focus on the strong positive anomalies. The characteristic precipitation pattern exhibits a meridional dipole structure with 37°N as the nodal latitude.

c. GPLLJ: Influence of ENSO and NAO

The ENSO and NAO impacts on the GPLLJ are examined from their contributions to the 900-hPa meridional wind in the 25°–35°N latitude band. The contributions are diagnosed in the same manner as those of the precipitation and are shown later (Fig. 10). Interestingly, many of the jet evolution features have correspondence in the precipitation evolution, which is not surprising, given the dominance of the transported moisture in the Great Plains precipitation variability. The evolution and intensity of the jet anomaly (top left, Fig. 10) closely matches the precipitation distribution (cf. Fig. 9, and likewise for the ENSO and NAO jet contributions. The GPLLJ anomalies are however positioned to the west of their precipitation contributions, much as in the climatology (Fig. 2). The residual jet (bottom left, Fig. 2), obtained after removal of the NAO and ENSO contributions, consists of a well-defined meridional wind pulse lasting a week to 10 days. The ENSO and NAO jet contributions evidently strengthen and effectively extend the pulse duration.

6. Remote influences

The large-scale upper-tropospheric circulation anomalies influential on Great Plains precipitation are examined here to advance our understanding of how the ENSO and NAO impacts are realized. The pentad resolution anomalies attributed to ENSO and NAO variability are identified using index regressions, as before.

The top panel in Fig. 11 shows the full 200-hPa height anomaly for June 1993, from the NCEP–NCAR reanalysis. This period is just prior to the wet episode and the NAO and ENSO contributions are identified to understand the setup for the extreme precipitation anomalies in early July. The monthly anomaly includes a zonally extended negative height anomaly northward of 30°N, with strongest amplitudes over the central Pacific. Geostrophic considerations suggest that the upper-level zonal flow was enhanced in the 30°–40°N belt, all the way up to the Rockies in June. Mo et al. (1995) implicate the stronger westerlies upstream of the mountains in the generation of the wet episode.

The middle panels in Fig. 11 show the ENSO and NAO contributions to the June 1993 height anomalies. Immediately apparent is a robust ENSO connection and the lack of an NAO link. The ENSO contribution over North America—a low stretching from the Pacific coast to the Hudson Bay—has an amplitude of up to 50 m, which is quite significant, within the context of summer stationary wave variability. This anomaly would be conducive for cyclogenesis in the lee of the Rockies and, thus, wetness over the Great Plains. Also notable in the

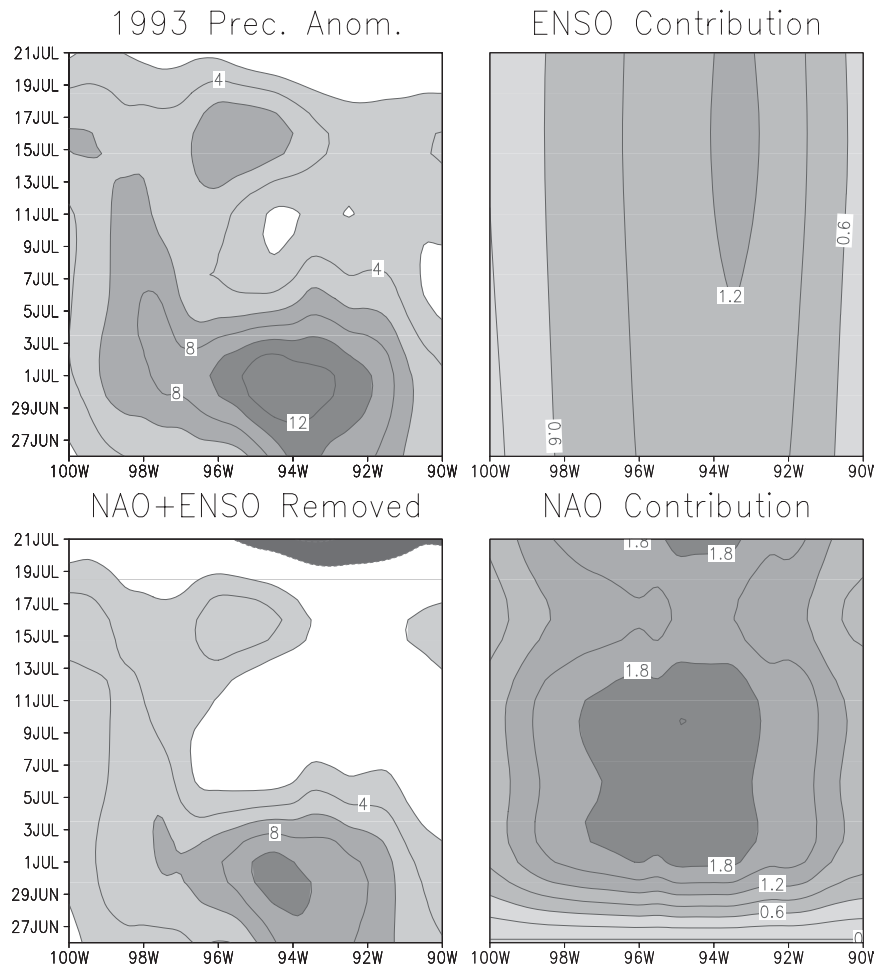


FIG. 9. Contribution by the NAO and ENSO to the pentad evolution of the July 1993 precipitation anomaly in NARR. (top left) The total anomaly, (bottom left) the total anomaly minus the combination of the NAO and ENSO precipitation footprint, and the (top right) ENSO and (bottom right) NAO contributions to the total anomaly. The contour interval for the left panels is 2 mm day^{-1} and for the right it is 0.3 mm day^{-1} .

ENSO contribution is the negative height anomaly found in the NAO region. Could this lead to NAO development in July? Compo et al. (2001) have noted the rather different high- and low-frequency ENSO circulation responses over the North Atlantic in winter, but the summertime differences remain to be characterized. The residual anomaly (Fig. 11, bottom) remains sizeable over many regions, including the Atlantic, but not over the North American continent where the deep trough is no longer in evidence.

Figure 12 shows the corresponding anomalies in July 1993, beginning with the full circulation anomaly, which is more wavelike than June's. The negative height anomaly over western North America has strengthened considerably, and is now flanked by two positive height anomalies to the east and west. This three-cell pattern has been noted within the context of enhanced sum-

mer-time precipitation over the central United States, most recently in WN.

The ENSO and NAO contributions to the July height anomaly are shown in the middle panels of Fig. 11. The much larger (and dominant) NAO signal is immediately apparent, as is the broad similarity of the June and July ENSO influence; the latter, in view of ENSO's long time scales. The NAO impact in July is robust, especially when compared to the nonexistent June signal. More importantly, the NAO is the dominant contributor to the structure and magnitude of the three-cell pattern (eastern North Pacific–western North America–eastern North America) save for the negative height anomaly over western North America, which are comparable to the ENSO contribution. Interestingly, the residual anomaly, obtained after the removal of both ENSO and NAO influences, still contains vestiges of the aforementioned

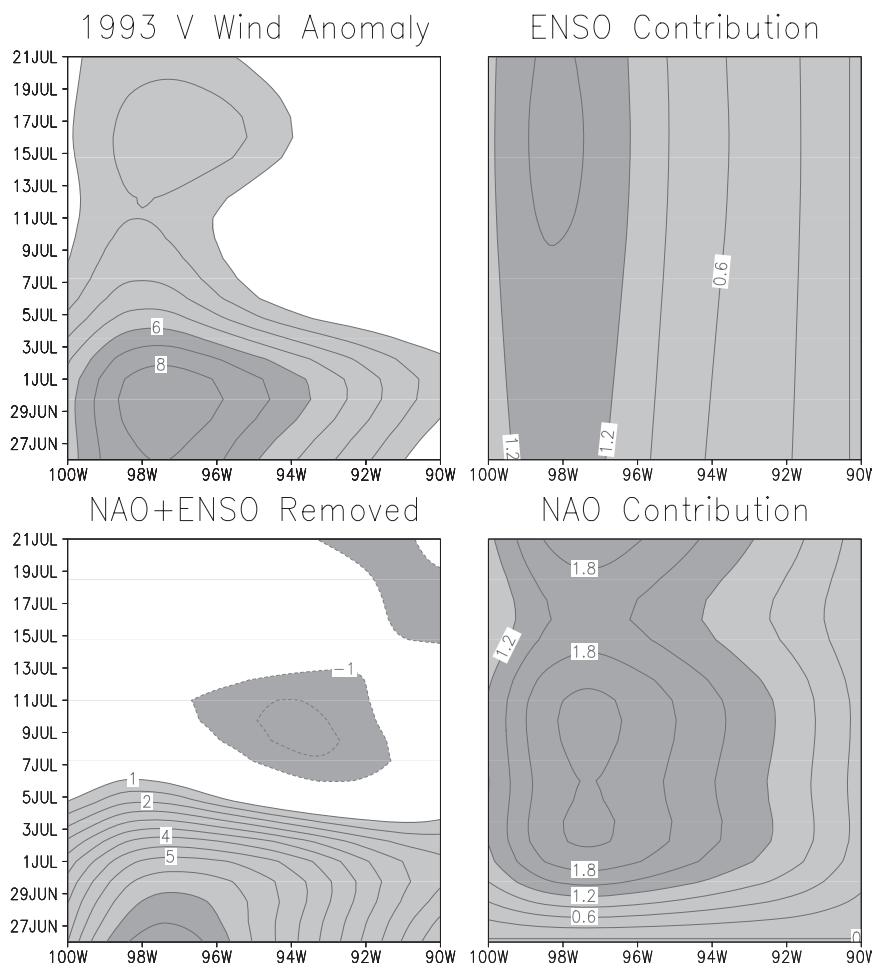


FIG. 10. Contribution by the NAO and ENSO to the pentad evolution of the July 1993 meridional wind anomaly in NARR. (top left) The total anomaly, (bottom left) the total anomaly minus the combination of the NAO and ENSO meridional wind footprint, and the (top right) ENSO and (bottom right) NAO contributions to the total anomaly. The contour interval for the left panels is 1 m s^{-1} and for the right it is 0.3 m s^{-1} .

three-cell pattern, thus retaining its influence on central U.S. precipitation.

As interesting and influential as the ENSO and NAO impacts are, especially, in prolonging one of the wettest Great Plains episodes in the modern record, the residual GPLLJ and precipitation anomalies remain substantial and consequential, attesting to the difficulties in predicting Great Plains rainfall. The large-scale circulation influences are considerably more notable in the upper-level height field, though, and how these can be tapped to advance predictability of Great Plains hydroclimate will be a subject of future investigation.

7. Discussion

The drought of 1988 and flood of 1993 have been analyzed in the North American Regional Reanalysis (NARR)—a high-resolution precipitation assimilating

dataset. Pentad evolution of the atmospheric and terrestrial based hydroclimate anomalies is analyzed to illuminate the pertinent temporal phase relationships of land–atmosphere interactions and large-scale and regional circulation patterns during these two extreme hydroclimate events.

The simultaneous analysis of the atmospheric and terrestrial water balances at pentad resolution provides a unique perspective, connecting canonical analyses of monthly hydroclimate anomalies with the inherent synoptic–supersynoptic circulation variability. The portrayal of water balance evolutions and the deduced nature of the balances demonstrate the important roles of circulation and transported moisture at supersynoptic time scales.

It is found that submonthly (but supersynoptic) time-scale fluctuations of the GPLLJ are the primary instigation

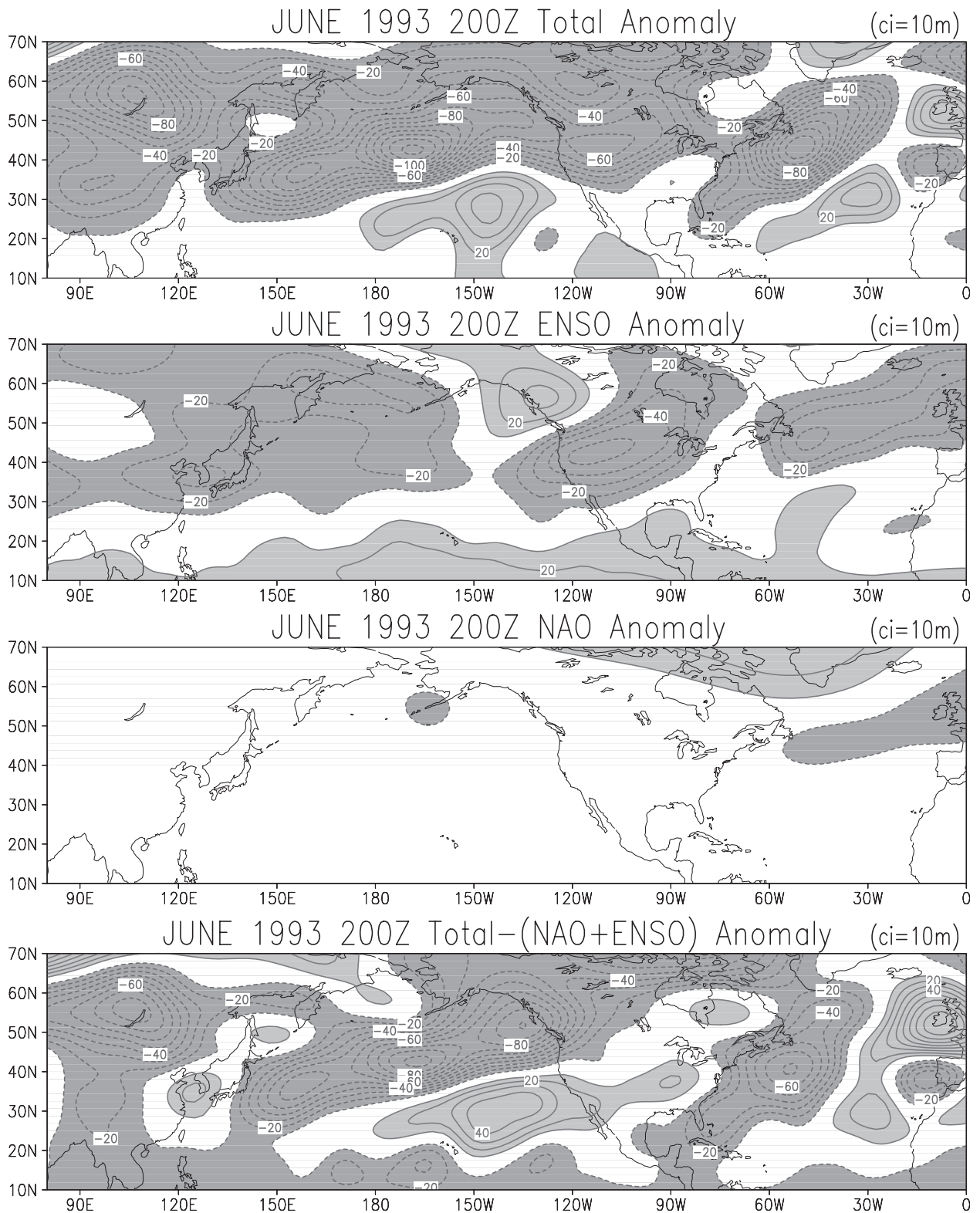


FIG. 11. Contribution of the NAO and ENSO to the 200-hPa height anomalies during June 1993. Positive (solid) and negative (dashed) anomalies are contoured at 10-m intervals. The total anomaly is in the top panel followed by the ENSO, NAO, and the total minus NAO + ENSO, respectively.

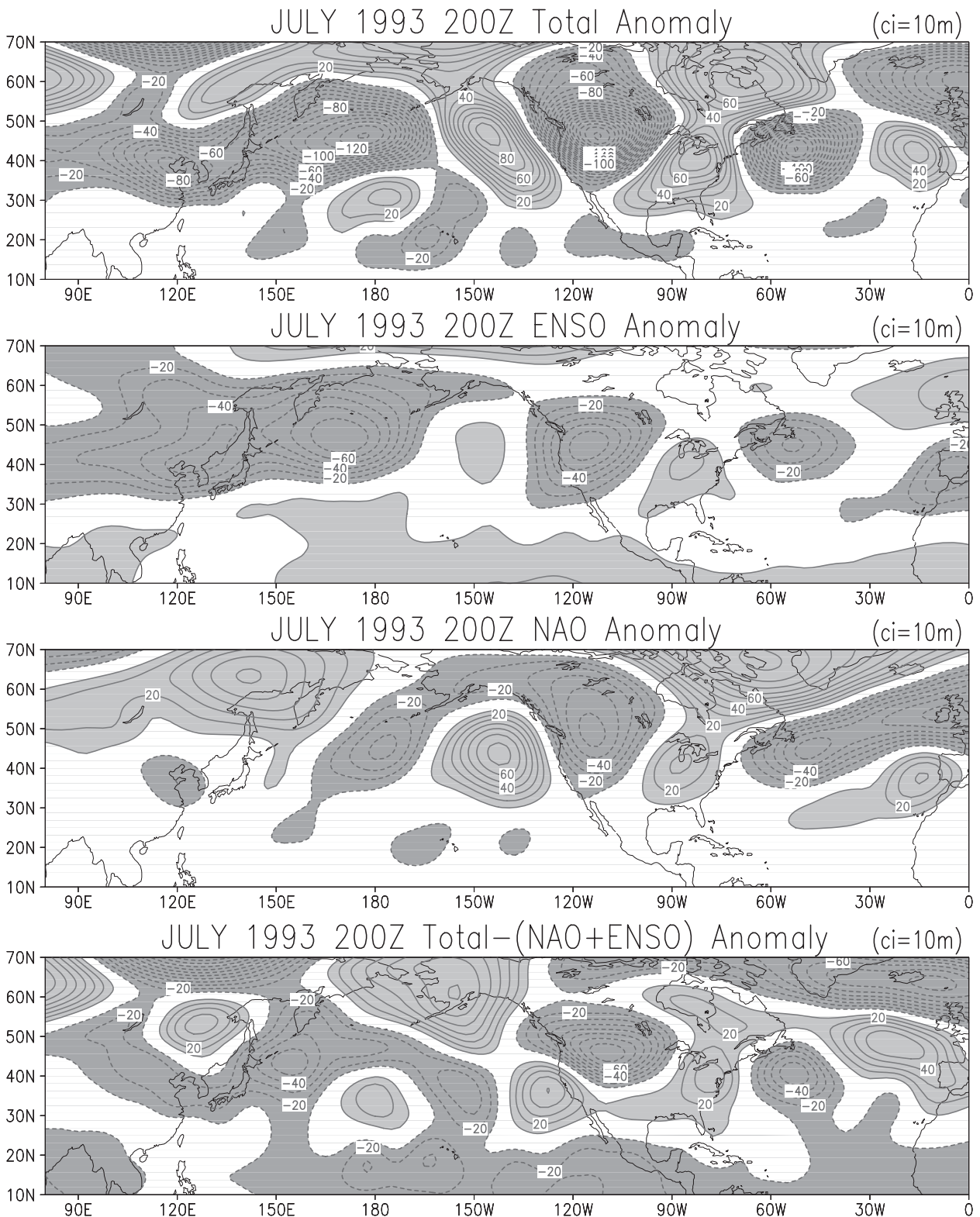


FIG. 12. As in Fig. 11, but for July 1993.

mechanism during these extreme events through their related moisture transport and kinematic convergence (i.e., $\partial v/\partial y$). The influential jet anomalies lead the moisture flux convergence by one pentad, which can account for two-thirds of the dry and wet episode precipitation amplitudes during the summers of 1988 and 1993.

Soil moisture influence on the evolution of hydroclimate anomalies is ascertained to be marginal. In the submonthly analysis, evaporation anomalies are found to lag precipitation ones, a lead-lag relationship not clear at monthly resolution. The regional atmospheric and terrestrial water budgets are unbalanced with the terrestrial *imbalance* significantly large. The sluggishness of the NARR evaporation (and overestimation during the wet period) is responsible for the atmospheric imbalance. The origin of the larger terrestrial imbalance resides in the unresponsiveness of the NARR's runoff, which is underestimated in the wet episode.

While the NARR is deemed a high-quality dataset for hydroclimate research due to the successful assimilation of observed precipitation (Mesinger et al. 2006), it is not immune to errors given its dependence on model physics parameterizations and potential observational errors. This may not be trivial in its portrayal of *unbalanced* water budgets and especially with respect to the terrestrial water budget, given the strong model dependence there. Shortcomings in the atmospheric water budget in the NARR have been noted previously, most recently by Nigam and Ruiz-Barradas (2006). Notwithstanding the lack of budget closures in the NARR, there is no escaping the conclusion that precipitation variations during the summers of 1988 and 1993 over the Great Plains are by and large consistent with moisture-flux convergence (MFC) variations in the overlying atmospheric column, especially given the large amplitudes of the observationally constrained and circulation-based (i.e., the GPLLJ and MFC) anomalies. At least over the Great Plains, these findings suggest a rather limited role of antecedent soil moisture anomalies, especially as the local supplier of moisture. Luo et al. (2007) have recently documented the soil moisture-precipitation lag correlation at monthly resolution for JJAS in 24 yr of NARR data. Their findings that no meaningful lag correlations exist between soil moisture (for both 0–10- and 0–100-cm layers) and precipitation over the upper Mississippi and Ohio basins further corroborates the results herein.

Given the prominence of transported moisture and large-scale circulation variability in generating these anomalous hydroclimate episodes (via GPLLJ-enhanced moisture flux convergence), the effects that the ENSO and NAO climate variability modes had on the regional low-level circulation and precipitation variations during

1993 are examined as a case study. The analysis shows that the ENSO contribution is long lived and provides a large portion of the antecedent (June 1993) large-scale circulation anomaly over the continental United States and North Atlantic, while the NAO's circulation influence is most notable during July 1993 and contemporaneous to the most extreme precipitation event.

The ENSO-NAO influence on regional GPLLJ and precipitation anomalies demonstrates interesting submonthly evolution, most notably with respect to the NAO. The ENSO contribution to the GPLLJ and precipitation anomalies exhibits temporal stability, which is not surprising given ENSO's strong persistence at submonthly time scales, while that of the NAO is slightly lagged—an interesting finding, and one that would not be discernible at monthly resolution. Together, the NAO and ENSO contributions account for ~25% of the precipitation and GPLLJ anomalies during 1993.

This study has demonstrated the complexity of the rapid circulation and land surface evolution in providing the necessary conditions for extreme hydrologic events over the Great Plains. Attribution of the mechanisms involved in producing extreme hydroclimate episodes is the subject of ongoing research and is predicated on lead-lag principal component regressions in extended EOF analysis. This will address the origin of the rapidly evolving variability structure and flesh out the competitive influences of the Great Plains soil moisture and large-scale remote circulation variability modes (i.e., ENSO-NAO).

Acknowledgments. The authors acknowledge support of NSF, NOAA, and DOE grants (ATM-0649666, CPPA NA17EC1483, and DEFG0208ER64548, respectively). The authors also thank Dr. Anthony Del Genio and two anonymous reviewers for their constructive comments.

REFERENCES

- Atlas, R., N. Wolfson, and J. Terry, 1993: The effect of SST and soil moisture anomalies on GLA model simulations of the 1988 U.S. summer drought. *J. Climate*, **6**, 2034–2048.
- Bates, G. T., and M. P. Hoerling, 2001: Central U.S. springtime precipitation extremes: Teleconnections and relationships with sea surface temperature. *J. Climate*, **14**, 3751–3766.
- Bell, G. D., and J. E. Janowiak, 1995: Atmospheric circulation associated with the Midwest floods of 1993. *Bull. Amer. Meteor. Soc.*, **76**, 681–695.
- Benedict, J. J., S. Lee, and S. B. Feldstein, 2004: Synoptic view of the North Atlantic Oscillation. *J. Atmos. Sci.*, **61**, 121–144.
- Bosilovich, M. G., and W. Y. Sun, 1999: Numerical simulations of the 1993 Midwestern flood: Land-atmosphere interactions. *J. Climate*, **12**, 1490–1505.
- Byerle, L. A., and J. Paegle, 2003: Modulation of the Great Plains low-level jet and moisture transports by orography and

- large-scale circulations. *J. Geophys. Res.*, **108**, 8611, doi:10.1029/2002JD003005.
- Carbone, R. E., J. D. Tuttle, D. A. Ahijevych, and S. B. Trier, 2002: Inferences of predictability associated with warm season precipitation episodes. *J. Atmos. Sci.*, **59**, 2022–2056.
- Compo, G. P., P. D. Sardeshmukh, and C. Penland, 2001: Changes of subseasonal variability associated with El Niño. *J. Climate*, **14**, 3356–3374.
- Ek, M. B., and Coauthors, 2003: Implementation of NOAA land-surface model advances in NCEP operational mesoscale Eta Model. *J. Geophys. Res.*, **108**, 8851, doi:10.1029/2002JD003296.
- Franzke, C., S. Lee, and S. B. Feldstein, 2004: Is the North Atlantic Oscillation a breaking wave? *J. Atmos. Sci.*, **61**, 145–160.
- Higgins, R. W., Y. Yao, and X. L. Wang, 1997a: Influence of North American monsoon system on the U.S. summer precipitation regime. *J. Climate*, **10**, 2600–2622.
- , —, E. S. Yarosh, J. E. Janowiak, and K. C. Mo, 1997b: Influence of the Great Plains low-level jet on summertime precipitation and moisture transport over the central United States. *J. Climate*, **10**, 481–507.
- Hong, S. Y., and E. Kalnay, 2002: The 1998 Oklahoma–Texas drought: Mechanistic experiments with NCEP global and regional models. *J. Climate*, **15**, 945–963.
- Hu, Q., and S. Feng, 2001: Variations of teleconnection of ENSO and interannual variation in summer rainfall in the central United States. *J. Climate*, **14**, 2469–2480.
- Kalnay, E., and Coauthors, 1996: The NCEP/NCAR 40-Year Reanalysis Project. *Bull. Amer. Meteor. Soc.*, **77**, 437–471.
- Liu, A. Z., M. Ting, and H. Wang, 1998: Maintenance of circulation anomalies during the 1988 drought and 1993 floods over the United States. *J. Atmos. Sci.*, **55**, 2810–2832.
- Luo, Y., E. H. Berbery, K. E. Mitchell, and A. K. Betts, 2007: Relationships between land surface and near-surface atmospheric variables in the NCEP North American Regional Reanalysis. *J. Hydrometeor.*, **8**, 1184–1203.
- Mesinger, F., and Coauthors, 2006: North American Regional Reanalysis. *Bull. Amer. Meteor. Soc.*, **87**, 343–360.
- Mo, K. C., J. Nogues-Paegle, and J. Paegle, 1995: Physical mechanisms of the 1993 summer floods. *J. Atmos. Sci.*, **52**, 879–895.
- , —, and W. Higgins, 1997: Atmospheric processes associated with summer floods and droughts in the central United States. *J. Climate*, **10**, 3028–3046.
- Namias, J., 1991: Spring and summer 1988 drought over the contiguous United States—Causes and prediction. *J. Climate*, **4**, 54–65.
- Nigam, S., and A. Ruiz-Barradas, 2006: Seasonal hydroclimate variability over North America in global and regional reanalyses and AMIP simulations: Varied representation. *J. Climate*, **19**, 815–837.
- Rasmusson, E. M., and T. H. Carpenter, 1982: Variations in tropical sea surface temperature and surface wind fields associated with the Southern Oscillation/El Niño. *Mon. Wea. Rev.*, **110**, 354–384.
- Ruiz-Barradas, A., and S. Nigam, 2005: Warm season rainfall variability over the U.S. Great Plains in observations, NCEP and ERA-40 reanalyses, and NCAR and NASA atmospheric model simulations. *J. Climate*, **18**, 1808–1830.
- , and —, 2006: IPCC's twentieth-century climate simulations: Varied representation of North American hydroclimate variability. *J. Climate*, **19**, 4041–4058.
- Sud, Y. C., D. M. Mocko, K.-M. Lau, and R. Atlas, 2003: Simulating the midwestern U.S. drought of 1988 with a GCM. *J. Climate*, **16**, 3946–3965.
- Trenberth, K. E., and G. W. Branstator, 1992: Issues in establishing causes of the 1988 drought over North America. *J. Climate*, **5**, 159–172.
- , and C. J. Guillemot, 1996: Physical processes in the 1988 drought and 1993 floods in North America. *J. Climate*, **9**, 1288–1298.
- , G. W. Branstator, and P. A. Arkin, 1988: Origins of the 1988 North American drought. *Science*, **242**, 1640–1644.
- Tuttle, J. D., and C. A. Davis, 2006: Corridors of warm season precipitation in the central United States. *Mon. Wea. Rev.*, **134**, 2297–2317.
- Weaver, S. J., and S. Nigam, 2008: Variability of the Great Plains low-level jet: Large-scale circulation context and hydroclimate impacts. *J. Climate*, **21**, 1532–1551.
- Zhang, D.-L., S. Zhang, and S. J. Weaver, 2006: Low-level jets over the mid-Atlantic region: Warm season climatology and a case study. *J. Appl. Meteor. Climatol.*, **45**, 194–209.